ACS APPLIED MATERIALS & INTERFACES

Research Article

www.acsami.org

Synthesis of Magnetic Rattle-Type Nanostructures for Use in Water Treatment

Stuart Linley,[†] Timothy Leshuk,[†] and Frank X. Gu*[,†,‡]

[†]Department of Chemical Engineering, [‡]Waterloo Institute for Nanotechnology, University of Waterloo, Waterloo, Ontario, Canada

Supporting Information

ABSTRACT: A hydrothermal technique to simultaneously remove a SiO_2 template and crystallize a TiO_2 outer layer was used to create magnetically separable, hollow rattle-type nanoparticles consisting of a magnetic Fe_3O_4 core contained within a hollow TiO_2 shell. Fe_3O_4 cores approximately 240 nm in diameter were synthesized, subsequently coated by SiO_2 and finally coated with TiO_2. This was followed by a hydrothermal treatment to selectively etch the silica, resulting in rattle-type particles with a final outer shell diameter of approximately 390 nm. The product of hydrothermal treatment were rattle-type particles with increased crystallinity and a 68% increase in surface area. Characterization confirmed the ability to etch a hard SiO_2 template through use of a simple and benign thermal treatment with pure water, while simultaneously introducing a crystalline phase into the TiO_2 active layer. The potential of the particles to be employed as a catalyst in UV induced advanced water treatment for removal of organic contaminants was evaluated through a colorimetric photocatalytic degradation assay using methylene blue as a model contaminant. The ability of the particles to be magnetically separated from solution after treatment and recycled for consecutive treatment cycles was then demonstrated. This technique for selectively removing a hard SiO_2 template while simultaneously crystallizing a TiO_2 shell avoids the use of hazardous chemical etchants or complex processing, rendering the synthesis of hierarchical, multimaterial, hollow, porous rattle-type particles a simple, attractive, and environmentally friendly "one-pot" technique for potential industrial application.

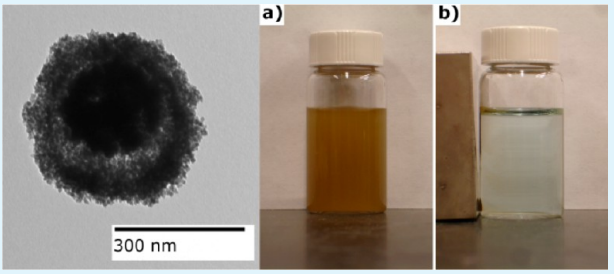

KEYWORDS: *hydrothermal, superparamagnetic, photocatalysis, green chemistry, hollow*

1. INTRODUCTION

Titanium dioxide has long been studied for its photocatalytic ability to stimulate the degradation of organic materials in water.[1] This property, coupled with its low cost and high efficiency has made TiO_2 a subject of much interest over the last few decades, particularly in the area of wastewater remediation.[2,3] The emergence of pharmaceutical contaminants and the presence of pathogens recalcitrant to traditional water treatment methods mandates water remediation techniques capable of dealing with such threats,[4−6] and TiO_2-based photocatalysis is a promising platform for addressing this issue.[7,8] Despite TiO_2's capability to remove most organic pollutants from water,[9,10] the problem of recovering the material after treatment still remains and presents potential hazards to aqueous ecosystems.[8] Many approaches have been investigated to solve this issue, including the deposition of TiO_2 onto various substrates such as sand, polymer beads, or magnetic cores. This enables easy, effective separation after water treatment with the additional benefit of being able to reuse the catalyst in subsequent water purification trials.[11−14] Ideally, such structures would have as much exposed surface area as possible to provide more catalytic reaction sites, making nanostructured particles an attractive option due to their high specific surface area. The combination of high surface area and easy separation is well embodied by magnetically separable nanoparticles that act as a platform for photocatalytic materials. Promising research into nanostructured catalysts with magnetic cores has shown that particles are easily recoverable in a matter of minutes.[15] Furthermore, careful design and testing of magnetic nanostructures has proven that catalysts can be collected and recycled for future use.[16,17] Liu et al. demonstrated this recently using zinc oxide nanoflakes on hollow, magnetic iron sulphide which showed no loss in activity after numerous photodegradation tests in the presence of methylene blue.[16] An additional technique for improving catalyst activity manifests itself in the form of hollow nanostructuring. The inclusion of hollow structure to catalyst particles provides additional surface area, more active sites, and lower density. This type of structuring for TiO_2 has been the focus of much attention as its light harvesting and photocatalytic properties are greatly improved over nonhollow particles.[18−20]

In this work, we sought to combine the important feature of magnetic separability for easy particle removal and recycling with the benefits of hollow TiO_2 structures to create an efficient, reusable nanostructured photocatalyst. In fact,

Received: December 14, 2012
Accepted: March 7, 2013
Published: March 7, 2013

previous work has shown that magnetic rattle-type nanostructures can be produced with exceptionally high surface areas, provided by the hollow shell, giving the material excellent adsorption properties. When this high surface area structure is combined with a magnetic core, the particles become highly functional; they have the ability to quickly adsorb contaminants and can be easily recovered from solution.[21,22] Hollow sphere structured TiO_2 provides significant benefits to the photocatalytic process in the form of higher surface area, better light harvesting capability, and the ability for pollutants to interact with both the interior and exterior of the shell.[19,23] By including a magnetic core in a rattle-type structure, all of the benefits of hollow TiO_2 spheres are retained, while also endowing the particles with magnetic separability. Various methods have been investigated for producing hollow- and rattle-type nanostructures, generally involving the use of a template which is removed in a final step to produce a hollow structure.[18,24] Indeed, previous works have demonstrated the synthesis of magnetic rattle-type TiO_2 structures; however, the synthesis methods typically involve organic templates, hazardous precursors, or dangerous etchants which we sought to avoid.[25,26] In this work, silica was chosen as template and spacer to separate the magnetic core and TiO_2 shell due to its straightforward surface deposition chemistry compatible with both of these oxide materials.[27−29] A hydrothermal technique for selectively removing this silica template while simultaneously introducing porosity and a phase change to anatase to the TiO_2 outer shell was proposed for the final production of rattle-type nanostructures consisting of a TiO_2 shell with a magnetic core. This technique offers the benefits of a simple, "green" water-based synthesis route through alleviating the need for dangerous chemical etchants as well as organic template materials which can be difficult to coat onto an inorganic substrate. Overall, this simple technique seeks to provide an environmentally friendly, efficient method for producing rattle-type structures which typically require a more complex synthesis route.

2. EXPERIMENTAL SECTION

2.1. Materials. Iron(III) chloride (99%, Sigma), tetraethyl orthosilicate (TEOS) (99%, Sigma), titanium(IV) butoxide (TBOT) (97%, Sigma) were purchased as precursors for each reaction step and used without further purification. Sodium citrate dihydrate (99%, Sigma), polyacrylamide (5−6 000 000 MW, Acros), ammonium hydroxide (28% solution, Sigma), ethanol (EtOH) (99%, ACS), methylene blue (Met-B) (>96%, Sigma), and hydroxypropyl cellulose (100 000 MW, sigma) were purchased and used without further purification.

2.2. Magnetic Core Synthesis. Controlled aggregates of Fe_3O_4 particles were synthesized according to a method modified from Cheng et al.[30,31] Briefly, sodium citrate dihydrate (70 mmol/L), urea (150 mmol/L), polyacrylamide (7.5 mg/mL), and iron(III) chloride (25 mmol/L) were added to 15 mL of Millipore water to prepare a mixed aqueous solution. This solution was sonicated at 60W (Branson Digital Sonifier 450, USA) for an hour to ensure the dissolution of the polyacrylamide. After sonication, the solution was transferred to a 23 mL Teflon lined stainless steel autoclave and hydrothermally treated at 200 °C for 12 h. The product was decanted into a 20 mL vial and washed by magnetic decantation three times with Millipore deionized water followed by three times with EtOH. The product was then dried in an oven at 70 °C for 2 h before being used in the next step.

2.3. Silica Coating. Magnetic cores as previously synthesized were coated with a silicon dioxide shell via a Stöber sol−gel reaction. Magnetic cores were weighed and added to a solution of EtOH, Millipore deionized water (12 mol/L), and ammonium hydroxide (0.15 mol/L) such that the concentration of magnetic cores was 1.5 mg/mL. This solution was sonicated at 40 W for 10 min to ensure good dispersion of particles. The solution was then decanted to a centrifuge tube and set vortex mixing. Three additions of 1 mol/L TEOS solution were made over 1 h (1 addition every 20 min) so that the final concentration of TEOS in the reaction vessel was 50 mmol/L. The solution was allowed to mix for 18 h overnight before being washed three times with EtOH by magnetic decantation the following day and finally dried before further use.

2.4. Titanium Dioxide Coating. The SiO_2 coated particles were coated in titanium dioxide via a sol−gel reaction.[32,33] Silica coated particles and hydroxypropyl cellulose (5 mg/mL) were dispersed in 10 mL of EtOH by ultrasonic agitation. In a round-bottom flask, a solution of Millipore deionized water (0.12 mL) and EtOH (15 mL) was prepared. After sonication, the dispersion was added to the round-bottom flask under vigorous mechanical agitation. A 0.12 mol/L solution of TBOT in EtOH was prepared in a small vial, and 5 mL was added dropwise to the round-bottom flask under vigorous agitation such that the final concentration of TBOT in solution was 20 mmol/L. This solution was then placed in an oil bath at 85 °C for 90 min under cold water reflux and vigorous agitation. After 90 min in the oil bath, the product was washed with EtOH three times by magnetic decantation and then dried in an oven at 70 °C over 2 h. This TiO_2 coating process was repeated once more using the previously-TiO_2-coated particles as seeds in order to achieve greater coating thickness.

2.5. Hydrothermal Treatment. The SiO_2 spacer shell of the composite particles was removed via a hydrothermal process. The same process served to promote a phase change of TiO_2 to anatase. The previously synthesized TiO_2 coated particles were dispersed in 30 mL of Millipore deionized water by ultrasonic agitation (40 W, 10 min) at a concentration of 1 mg/mL and then added to a 45 mL Teflon lined stainless steel autoclave and heated to 180 °C for 1.5 h. The product was washed with Millipore deionized water three times by magnetic decantation and then either dried for characterization or left dispersed in water for photocatalytic testing.

2.6. Photocatalytic Removal of Methylene Blue. The photocatalytic reactions were performed in 50 mL Pyrex beakers pretreated with chlorotrimethylsilane to make them hydrophobic. Each beaker contained 20 mL of reaction slurry (1 mg/L methylene blue, 0.1 mg/mL catalyst particles). The solution was mixed and then placed under a UV light source (UVP, CL-1000) with maximum output at a wavelength of 254 nm . Tests were done at an intensity of 0.8 W/cm^2. One milliliter aliquots of the slurry were drawn at predetermined time intervals and analyzed by a microplate spectrophotometer (BioTek Epoch Take 3, USA). Spectrometric measurements were taken at 668 nm as this was found to be the peak absorption wavelength of methylene blue. Particles were separated from the slurry by centrifugation at 15 000 rpm for 15 min to ensure the absence of composite particle in spectrometric analysis.

For the recyclability study, the reaction slurry was made up as above using 1 mg/L methylene blue and 0.2 mg/mL catalyst particles. The solution was exposed to UV light, and readings were taken after each 30 min period. At these points, photocatalysts were magnetically separated from solution and the supernatant was replaced with fresh 1 mg/L Met-B solution. After 5 h catalysis trials, the particles were suspended in Millipore water and exposed to a 9W UV light source (Philips, PL-S9W UV-A) overnight (18 h exposure). Following this overnight UV exposure, the water was replaced with methylene blue solution as previously described, and testing continued as before. Samples were spectrophotometrically analyzed as described previously.

2.7. Characterization. The size and surface morphology of the particles were analyzed with a Philips CM-10 transmission electron microscope (TEM). Samples were prepared by placing 5 μL of aqueous solution containing photocatalysts on Formvar-carbon coated 100 mesh copper TEM grids (Canemco) and allowed to dry overnight in a covered Petri dish. Scanning electron microscope (SEM) characterization was performed using a FEI Magellan 400 XHR-FEGSEM. All images were taken at a 2 kV acceleration voltage. Energy dispersive X-ray spectroscopy (EDX) and selected area electron diffraction (SAED) measurements were taken using a FEI TITAN LB

80−300 HRTEM. Surface area of the materials was determined using the Brunauer-Emmet-Teller (BET) equation with data obtained from N_2 adsorption isotherms taken at 77 K by a Gemini VII 2390 surface area analyzer. X-ray diffraction (XRD) data was obtained using an XRG 3000 X-ray diffractometer with a Cu Kα radiation source (λ = 1.5405 Å), and input voltage and current were set at 30 kV and 30 mA, respectively.

3. RESULTS AND DISCUSSION

A synthesis protocol to produce hollow, magnetically separable TiO_2 rattle-type particles was developed by sequentially coating various inorganic layers onto a core particle. The end goals of this process included greatly simplifying the synthesis procedure of such complex, hierarchical particulate structures, as well as reducing the costs associated with synthesis and making production of such particles as nontoxic and safe as possible by performing the template-removal step in pure water. It is well-known that hydrothermal treatment is capable of crystallizing TiO_2, and recent reports have shown that the same treatment can dissolve silica templates.[34,35] It was thought that use of hydrothermal processing could thus simultaneously eliminate the necessity for difficult organic templates or hazardous chemical etchants in the synthesis, as well as remove the need for further energy-intensive high temperature processing which is typically necessary to introduce crystallinity into the TiO_2 phase, thereby making the synthesis of such hierarchical functional materials both more economical and environmentally conscious.

3.1. Synthesis of Core−Shell Structure by Deposition of Silica Spacer on Magnetic Fe_3O_4 Cores. The first step of the synthesis process involved production of magnetic cores to endow the particles with magnetic separation capability. The material selected for this purpose was Fe_3O_4 since this is a highly magnetic phase of iron oxide and displays the property of superparamagnetism when the crystal grain size is ~20 nm, meaning the particles do not exhibit a permanent residual magnetic moment after exposure to a magnetic field.[36] Magnetite cores synthesized using a hydrothermal precipitation method can be seen in Figure 1a. The mean diameter of the cores was found to be 242 ± 21 nm determined by measuring sets of TEM images, examples of which are shown in Figure 1.

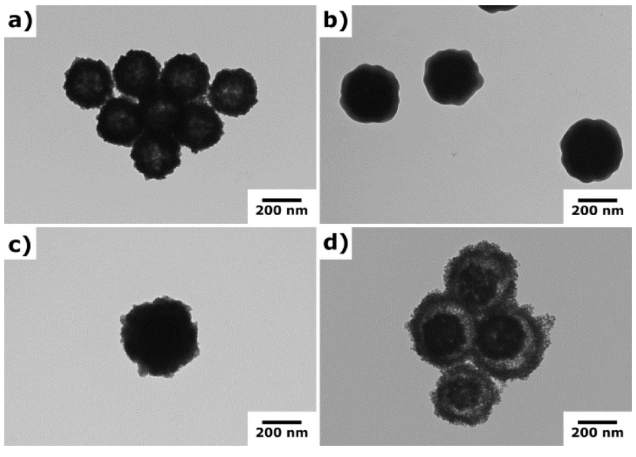

Figure 1. Transmission electron microscopy (TEM) images of the particles throughout various stages of synthesis: (a) Iron oxide Fe_3O_4 core particles, (b) core particles coated with SiO_2, (c) Fe_3O_4/SiO_2 particles coated with TiO_2, and (d) TiO_2/magnetic core rattle structures after hydrothermal treatment.

SEM characterization further demonstrates the spherical, monodisperse nature of the particles as seen in Figure 2a. Each

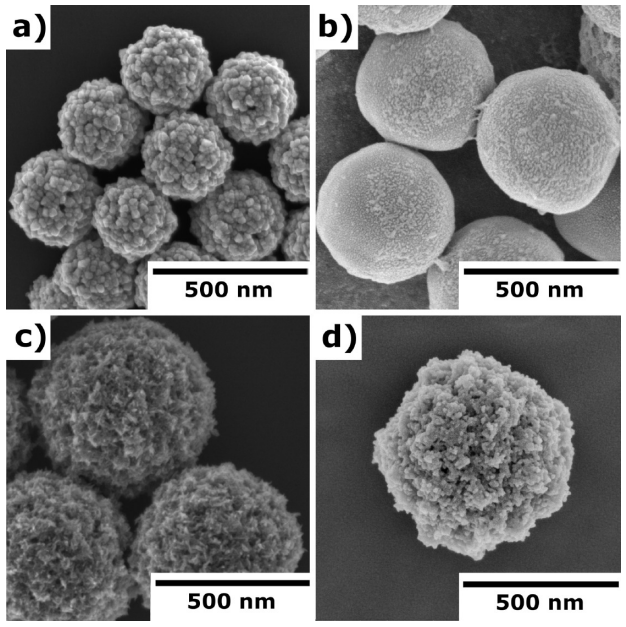

Figure 2. Scanning electron microscopy (SEM) images depicting the particles after different stages of synthesis: (a) Fe_3O_4 cores, (b) Fe_3O_4 cores coated with SiO_2, (c) Fe_3O_4/SiO_2 coated with TiO_2 after two coating procedures, and (d) magnetic rattle-type structures after hydrothermal treatment to remove SiO_2 layer.

of the core particles appears well formed and separate from its neighbors. As is evident in TEM and SEM images, the magnetite cores appear to be made up of many smaller magnetite nanocrystals, an observation confirmed by Cheng et al. where magnetite spheres made by the same method have a polycrystalline structure apparently composed of an aggregate of smaller Fe_3O_4 nanocrystals.[30,31] It is thought that the crystal growth in this mechanism is slowed due to coordination of metal ions by citrate and that the aggregation of nanocrystals into larger spheres occurs to minimize surface energy.[30] The aggregated nanocrystalline nature of these spheres provides two advantages to the final composite particle product. First, since the cores are aggregates of crystals with single magnetic domains, the material remains superparamagnetic, preventing interparticle magnetic aggregation. Second, the total magnetic force exerted by the sphere in a magnetic field is strong due to the simultaneous magnetization of many smaller grains. This allows for significant magnetic moment, resulting in quick separation even when loaded with multiple surface layers such as SiO_2 or TiO_2. When subjected to a magnetic field gradient, it was found that the particles had strong magnetophoretic response, separating from suspension within 1 min of magnet application to the external surface of the vial. Particles produced by a similar method were found to have no remnant magnetization or coercivity, properties characteristic of superparamagnetic particles less than 30 nm in size.[31] Furthermore, the spheres reported by Cheng et al. showed a high saturation magnetization attributed to the aggregation of many superparamagnetic grains into a single particle.[31] In addition to this, the size and morphology of the particles is comparable to results presented by Cheng et al. where the spheres are well

dispersed, have a narrow size distribution, and show a rough surface.[30,31]

To obtain a rattle-type structure, a spacer was coated onto the surface of the magnetite cores which would eventually be removed in a later step. Silica was chosen as a template material and coating of the magnetite cores was achieved by a modified Stöber method. The sol−gel method for depositing silica has been extensively studied for decades and is exceptionally compatible with hydrated iron oxide interfaces. Surface hydroxyls of the Fe_3O_4 can initiate the condensation reaction of the dissolved siliceous monomers, resulting in a controlled, conformal coating of amorphous silica commensurate with the contour of the seed oxide surface. As shown in Figures 1b and 2b, it can be observed that a conformal and smooth silica layer coats the outside of the particles when compared to the polycrystalline surface of the Fe_3O_4 aggregates observed in Figures 1a and 2a. Furthermore, SEM characterization provides further confirmation that the silica deposition coated individual particles rather than aggregates, as the particles visible in Figure 2b appear distinct from surrounding particles. Sizing from the TEM micrographs reveals that the silica coated particles are roughly 308 ± 29 nm in diameter, giving a SiO_2 shell thickness of approximately 34 nm. The thickness of this silica shell could be easily controlled and varied by simply changing the amount of TEOS added to the coating reaction.

3.2. Titanium Dioxide Deposition and Hydrothermal Treatment. In order to produce rattle-type particles, a hydrothermal process was used to selectively etch the silica template and crystallize the TiO_2 outer layer in a "one-pot" reaction. After performing the titanium dioxide coating procedure twice in sequence on these silica coated particles, the previously smooth surface appears roughened once again due to the deposition of amorphous TiO_2. This difference is clearly observable by comparing Figure 1c to Figure 1b and comparing Figure 2c to Figure 2b. Sizing data confirms that, after TiO_2 coating, the particles have a mean diameter of 383 ± 35 nm, yielding a TiO_2 shell thickness of approximately 37 nm. Once again, SEM characterization can further confirm that the particles are individually coated by TiO_2 and are observably monodisperse and spherical as seen in Figure 2c.

After hydrothermal treatment at 180 °C for 1.5 h, it is observable that the SiO_2 layer between the magnetite core and the TiO_2 shell has been removed (Figure 1d), while SEM characterization demonstrates that the spherical morphology and monodispersity of the particles has not been affected by hydrothermal treatment (Figure 2d). The removal of the silica spacer is consistent with literature where hollow spheres were synthesized by removing a hard SiO_2 template or dissolving cores of silica particles with hydrothermal treatment in nearly pH neutral environments.[35,37] The solubility and dissolution rate of silica is increased at high temperatures,[37] and by hydrothermally treating the templated particles, the spacer can be dissolved quickly, leaving a rattle-type structure. Since silica dissolution takes place by an equilibrium mechanism,[38] some SiO_2 is likely left on the outer and inner surfaces of the Fe_3O_4 and TiO_2, respectively. EDX characterization of the elemental composition of the particles, presented in Table 1, confirms the presence of Si after the hydrothermal treatment, which is likely due to the presence of residual SiO_2. However, the concentration of Si in the particles is substantially reduced by the hydrothermal treatment, from 25.5 to 6.3 at. %, in accordance with the dissolution of the majority of the SiO_2 spacer layer. The residual silica may, in fact, serve to enhance the photocatalytic properties of the TiO_2 by increasing surface area and surface acidity, as has been reported in a number of works.[39−41] To further study the localization of the residual or redeposited Si within the particle structure before and after hydrothermal treatment, an EDX line scan was performed on selected particles, as shown in Figure 3. The fluctuation in metallic atomic percentage evident in Figure 3a clearly demonstrates the $Fe_3O_4/SiO_2/TiO_2$ structure prior to hydrothermal treatment. The iron at. % is highest toward the center of the particle, where the iron oxide core would be, while the Ti at. % is greatest at the particle's outer shell. Figure 3a also clearly demonstrates that the Si at. % reaches a peak at the spacing between the iron oxide core and the titanium dioxide shell. Figure 3b shows the fluctuation in metallic at. % after hydrothermal treatment. Note that the Ti and Fe at. % distribution remains largely unchanged while the Si at. % is decreased throughout the entire particle. It can be concluded that the remaining Si detected by EDX is approximately uniformly distributed throughout the particles, possibly remaining in pores on the inner surfaces of the rattle structure, essentially as a residual background signal. Thus, EDX confirms the successful formation of the rattle structure by the dissolution of the SiO_2 spacer from the significant decrease in the Si signal following hydrothermal treatment.

Table 1. Elemental Composition (at %) of Samples before and after Hydrothermal Treatment, from EDX

element	prehydrothermal	posthydrothermal
Fe	15.70	23.04
Si	25.47	6.29
Ti	9.53	7.75
O	49.30	62.92

The surface roughness of the TiO_2 shell appears increased when comparing Figure 1d to Figure 1c and Figure 2d to Figure 2c, suggesting crystallization has occurred. It is known that the presence of water during the crystallization process of TiO_2 can significantly lower the temperatures required to achieve phase changes.[42,43]

Crystallization of TiO_2 by hydrothermal treatment is thought to occur in two steps; first, a fast nucleation of small anatase crystals from amorphous TiO_2 occurs, followed by a slow dissolution and deposition process.[43] The first phase of this crystallization process is thought to occur by solid state epitaxial growth, but after this short, fast growth process, the water present in hydrothermal treatment inhibits epitaxial growth, and further crystallization occurs through an in situ hydrolysis and condensation process using water as a catalyst.[43] Additionally, the observed surface roughness may indicate the presence of disordered pores in the TiO_2 material. A paper published by Li et al. presents the formation of mesoporous TiO_2 through a hydrothermal treatment process.[44] The pores appear through an Ostwald ripening process whereby smaller anatase crystals slowly disappear and enable the growth of larger crystals, leaving voids which contribute to surface roughness.[44]

The diameter of the TiO_2 shells after hydrothermal treatment was found to be 389 ± 39 nm indicating that no appreciable size change occurs due to hydrothermal treatment. Application of a permanent magnet to a dispersion of the hollow particles after hydrothermal treatment still elicits a strong response, with complete separation of particles from suspension in less than 1 min. The enhanced porosity of the

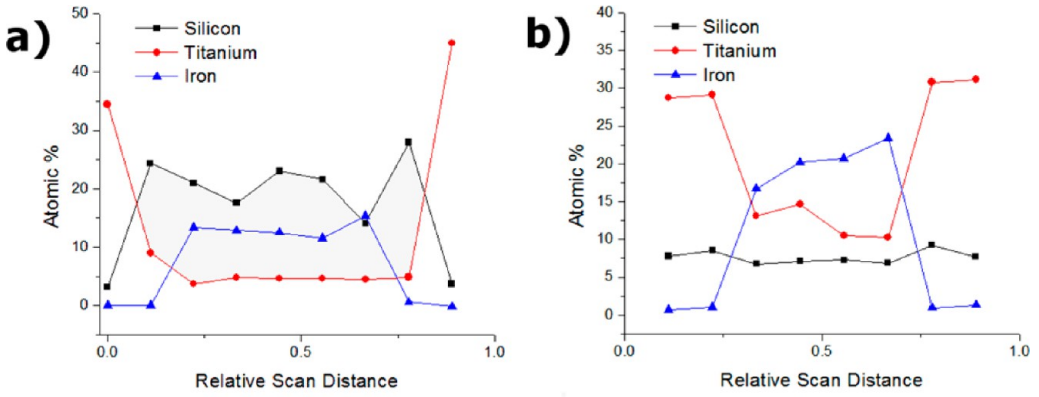

Figure 3. EDX line scan results of TiO_2 coated particles. The line scan path for both graphs extends along the diameter of a single particle, passing through the center. Each graph shows the metallic atomic % of the indicated element over a line scan of a particle before (a) and after (b) hydrothermal treatment. See Supporting Information for locations of EDX line scans.

TiO_2 shell, combined with the hollow nature of the TiO_2 shell, was expected to provide these particles with a superior surface area when compared to the nonhydrothermally treated particles presented in Figure 1c. TEM characterization demonstrates that the hydrothermal processing was successful in producing hollow, rattle-type particles as intended.

3.3. Confirmation of Properties after Hydrothermal Treatment. Previous studies indicate that hydrothermal treatment of TiO_2 yields anatase at relatively low temperatures and introduces pores to the material, increasing the surface area and providing more reactive sites.[34,45] The crystallization of TiO_2 under hydrothermal treatment is essential for transforming the amorphous TiO_2 material into the photocatalytically active anatase phase, while also reducing the processing time and energy consumed relative to standard calcination methods. Both crystallinity and porosity are essential for increasing the photocatalytic activity of the particles. Confirmation of these properties was obtained by conducting X-ray diffraction and SAED, and N_2 adsorption characterization to assess the crystallinity and surface area of the product, respectively.

The X-ray diffraction (XRD) spectra of the samples before and after hydrothermal treatment were analyzed to determine differences in the crystal structure of the TiO_2 shell, as well as to determine the phase of iron oxide present in the cores of the particles (Figure 4). The diffraction spectra shown in Figure 4a can be indexed to magnetite, Fe_3O_4 (JCPDS Card # 19-629), with no appearance of any peaks characteristic of TiO_2 or SiO_2 phases, indicating that both the silica and titania phases are amorphous before hydrothermal treatment. The pattern displayed in Figure 4b shows the same sample after hydrothermal treatment at 180 °C for 1.5 h. The appearance of new peaks in Figure 4b indicates a phase change in the TiO_2 outer shell as each of the new peaks can be indexed to the TiO_2 anatase phase (JCPDS Card # 21-1272). Additionally, HRTEM SAED characterization seen in Figure 5 further confirms the phase change of the TiO_2 from amorphous to anatase. The SAED diffraction pattern in Figure 5b shows no coherent scattering of electrons, indicating an amorphous material, while Figure 5d clearly shows a ring diffraction pattern characteristic of anatase TiO_2. The first four rings of the diffraction pattern of Figure 5d can be indexed to (101), (200), (004), and (105), starting from the center ring. The sampling locations for SAED can be seen in Figure 5a,c which also serve as a morphological comparison before and after hydrothermal treatment. The

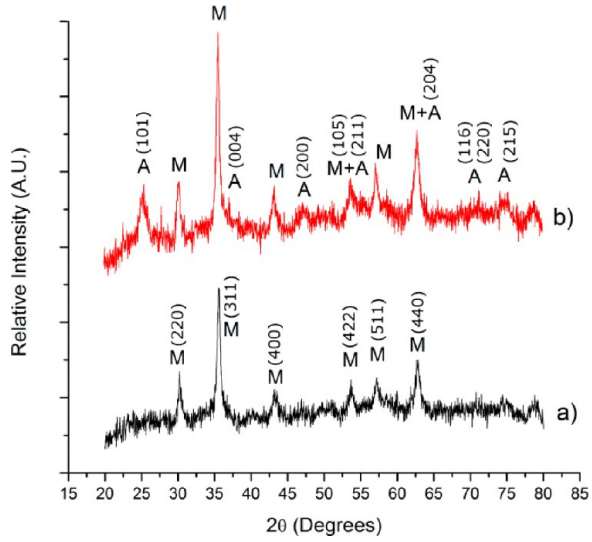

Figure 4. XRD results demonstrate the phase change of the TiO_2 shell of the rattle particles from amorphous to anatase. Spectrum (a) shows the particles prior to hydrothermal treatment. All crystalline planes indicated in spectrum (a) are for magnetite. Spectrum (b) shows the particles after hydrothermal treatment. All crystalline planes indicated in spectrum (b) are for anatase TiO_2. An "M" denotes a magnetite Fe_3O_4 peak; "A" denotes an anatase TiO_2 peak.

particles appear solid prior to hydrothermal treatment in Figure 5a and clearly have a rattle structure in Figure 5c indicated by the area of lower electron density surrounding the iron oxide core. Traditionally, TiO_2 requires high calcination temperatures of above 400 °C to achieve the phase change to anatase, but this change in crystallinity at a comparatively low temperature can be attributed to the high pressure environment of hydrothermal treatment and the effect of water on crystal growth.[42,43,45] The relatively low intensity of these anatase peaks is characteristic of hydrothermal crystallization, and previous studies have demonstrated that the crystallinity of TiO_2 is increased with higher temperature hydrothermal treatment and with longer hydrothermal treatment times.[45] In addition to this, the consistency of the magnetite peaks visible in Figure 4a,b suggests that the crystal phase of the iron oxide core has not been altered as a result of the hydrothermal treatment, explaining why the magnetic properties of the particles are not significantly affected.

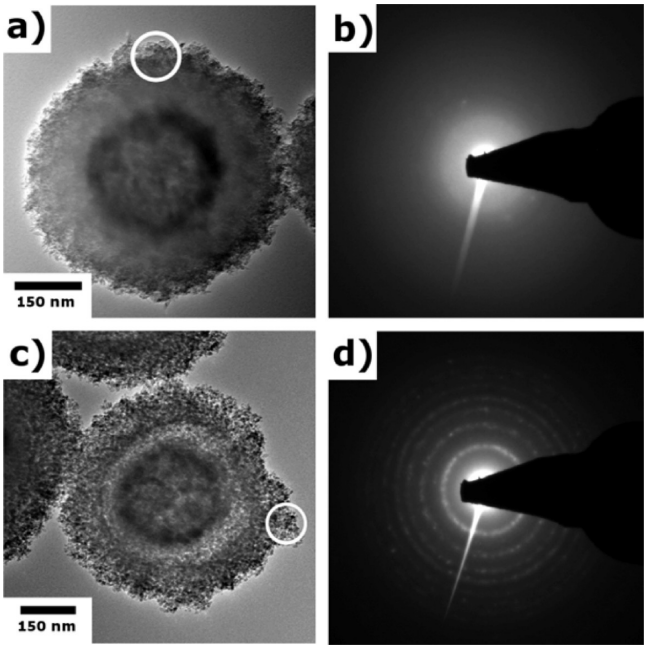

Figure 5. HRTEM and SAED characterization of the TiO_2 particles before and after hydrothermal treatment. Panels (a) and (c) demonstrate the morphology of the particle before and after hydrothermal treatment, respectively. The white circle highlights the selected area for electron diffraction. Panels (b) and (d) demonstrate the SAED pattern of the selected area before and after hydrothermal treatment, respectively.

It should be noted, however, that the XRD spectra of maghemite (γ-Fe_2O_3) (JCPDS Card # 39-1346) is nearly indistinguishable from that of magnetite and it is possible that partial oxidation of the cores to this phase occurred. This data, coupled with the information provided from TEM and SEM characterization, confirms that hydrothermal treatment can be used as a method for simultaneously removing a silica template and crystallizing TiO_2.

The Brunauer-Emmet-Teller equation was used in conjunction with N_2 adsorption isotherm in order to determine the surface areas of the particles before and after hydrothermal treatment. A significant increase in surface area as a result of hydrothermal treatment serves to demonstrate two key characteristics of the particles; first, it gives extra confirmation that the silica template has been removed from the particles, and second, it shows that the treated particles have more reaction sites for photocatalysis. BET surface area results demonstrated an approximate 68% increase in surface area between the sample before and after hydrothermal treatment. After the initial TiO_2 coating, N_2 adsorption revealed the specific surface area to be 61.40 ± 1.05 m^2/g. After removal of the silica template layer by hydrothermal treatment, the specific surface area was found to be 103.42 ± 0.53 m^2/g. The reason for the increase in surface area is most likely a combination of both an increasing and decreasing effect. Surface area is increased due to the removal of the silica template, allowing N_2 access to the inner shell of the particles, but simultaneously decreased due to an increase in crystallite size which is known to occur under hydrothermal calcination,[45] whereby the TiO_2 is densified and micropores characteristic of sol−gel-formed amorphous materials are eliminated.

In their comprehensive study of hydrothermal effects on TiO_2, Yu et al. found that longer hydrothermal treatment times and higher temperatures yielded larger crystallite sizes and lower specific surface areas.[43] By choosing a relatively short hydrothermal treatment time in this study, the loss in surface area due to crystallite formation was minimized while still introducing a phase change and removing the silica template. This analysis confirms that the hydrothermal treatment process improves surface area via removal of the silica template, while simultaneously crystallizing the TiO_2 shell.

3.4. Photocatalytic Activity and Recyclability of Particles. In order to assess the ability of the particles to be applied as a recyclable photocatalyst for advanced water treatment, degradation trials and a recyclability study were performed. Photocatalytic degradation trials were performed using methylene blue as a model contaminant to test the ability of the particles to remove an organic material from aqueous solution. Particles were tested at a methylene blue concentration of 1 mg/L and a nanoparticle loading of 0.1 mg/mL. At these loadings, the rattle-type particles were found to completely remove methylene blue from solution over a testing period of 10 min, as can be seen by the decrease in the methylene blue spectrum over time in Figure 6. The rattle

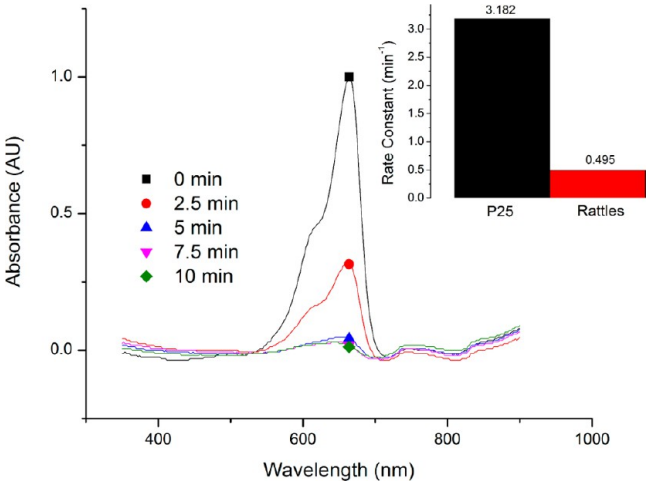

Figure 6. Photocatalytic degradation of methylene blue due to rattle particle interaction: The spectrum graph shows the rattle-type particles activity over time. The inset shows a comparison of the pseudo first order rate constants between Degussa P25 and the rattle particles.

particles were compared to Degussa P25 by performing an identical photocatalytic test using P25 and fitting a pseudo first order rate constant to an exponential trend. The rate constant for the rattle-type particles under these testing conditions was found to be 0.495 min^{-1}, while the rate constant for P25 was found to be 3.182 min^{-1}. Although P25 performed superior to the rattle-type particles, it should be noted that the comparison is done based on mass of particle in the reaction slurry. The rattle-type particles contain iron oxide cores and residual silica which add significantly to their mass while the P25 particles are pure TiO_2. This discrepancy could account for some of the significant difference in rate constant when compared to P25. Comparison by mass was chosen since neither the surface area nor mass of only the TiO_2 component could be accurately measured or estimated due to physical changes in the core materials from the hydrothermal treatment and porous nature of the TiO_2 shell. Additionally, the presence of an unshielded iron oxide core has been shown to promote electron−hole recombination with TiO_2, significantly decreasing the photo-

dx.doi.org/10.1021/am303117g | ACS Appl. Mater. Interfaces 2013, 5, 2540−2548

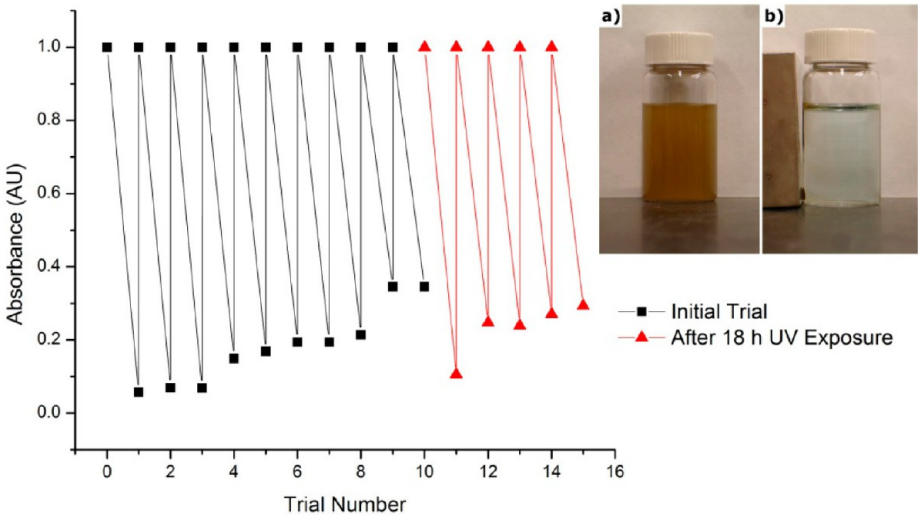

Figure 7. Repeated trials showed methylene blue removal from solution after 30 min UV irradiation per trial. The methylene blue concentration is 1 mg/L while the particle concentration is 0.2 mg/mL. ■: initial repeated trials; red ▲: repeated trials following 18 h exposure to a 9W UV-A bulb. See experimental Section 2.6 for more details. The inset demonstrates magnetic separability of the rattle-type particles: (a) Particles before application of magnetic field; (b) particles 1 min after application of magnetic field.

catalytic activity of the TiO_2 outer material.[46] Electronic contact between these two materials, once no longer separated by the SiO_2 middle layer, could be another significant factor attributing to the lower activity of the rattle particles compared to P25. In our previous work, hollow TiO_2 spheres made by a similar method showed photocatalytic activity exceeding that of P25,[47] indicating that the presence of a Fe_3O_4 core indeed does reduce photocatalytic efficiency. It should be noted, however, that the hollow TiO_2 spheres studied did not suffer TiO_2 mass discrepancies when compared to P25 as the material was pure TiO_2.[47] Ideally, to prevent electronic contact but maintain a rattle structure, a thin silica shell would remain coating the iron oxide core to prevent electronic contact between these materials. Previous findings indicate that this feature may be possible to attain using the synthesis technique outlined in this paper with some modifications to the hydrothermal treatment step, which can greatly influence the removal of silica.[47] Finally, it should be noted that photolysis of the dye due to UV irradiation over this time period was found to be negligible, indicating that dye removal was entirely due to presence of the particles in solution. Despite the difference in photocatalytic activity, the significance of the rattle design is demonstrated in the simple recovery of these particles for recycling, where in contrast P25 nanoparticles are very difficult and costly to completely remove from treated solution, and thus despite their high activity, are impractical for deployment as a photocatalytic slurry.

The rattle particles demonstrate better photocatalytic activity than TiO_2-coated magnetite particles which were only treated hydrothermally (without air calcination) in a recent study by Wu et al.[48] Their particles remove ~50% of methylene blue over a 90 min period[48] while the particles presented here show complete removal of the dye in approximately 5 min. This significant improvement in activity of the rattle particles can be attributed to their high surface area provided by their hollow structure, the crystal phase change of the TiO_2 layer to anatase (which is well-known to have superior photocatalytic performance over other phases of TiO_2), and better light harvesting by possible light reflection between the hollow shell and the core.[18,19] In addition to this, the presence of residual silicon dioxide may act to improve photocatalytic activity by causing an anodic shift of the TiO_2's conduction and valence bands, increasing its oxidation activity, and by introducing an energy barrier which inhibits recombination, preserving carrier lifetime.[40]

An important aspect of this synthesis technique is the ability to magnetically separate and recycle the particles for use in subsequent water treatment cycles, thereby reducing the cost and environmental impact of implementing this technology. Another important factor to consider is the ability to completely remove the particles from the treated water to prevent them from acting as contaminants themselves. In order to demonstrate the ability of these particles to be recycled for use in multiple trials, the same set of particles was used to degrade multiple batches of methylene blue solution consecutively. A nanoparticle/methylene blue solution was irradiated with UV light for 30 min; then, the nanoparticles were magnetically separated, and the test was repeated with fresh methylene blue. The results of this study can be seen in Figure 7. Initially, the catalyst was able to remove the dye from solution completely over the course of half an hour. After 10 trials (5 h continuous activity), it was found that the particles could only remove approximately 65% of the dye in solution; however, after overnight exposure to a 9W UV-A bulb, the particles were once again able to remove 90% of the dye in a 30 min period. The most likely explanation for this observation is methylene blue from previous tests saturating the catalyst active sites. Over the 5 h testing period, undegraded methylene blue may build up on the particle surface and prevent degradation of the fresh methylene blue in the replacement solution. The increased activity after a UV regeneration period supports this hypothesis. During the 18 h UV-A exposure, methylene blue on the particle surface is degraded and removed, freeing up catalyst active sites for the following trial. Thus, it is clear that the catalyst can be used for multiple trials without a large decrease in efficiency, and furthermore, it can be regenerated via a simple UV exposure. These results match expectations, as it has been shown that TiO_2 can be recycled for further use without decrease in catalytic efficiency as long as TiO_2 recovery is efficient.[48,49] Photocatalytic activity using the rattle-type

particles was not significantly hindered after multiple trials and returned to efficacy comparable to unused particles after 18 h UV-A exposure, indicating that TiO_2 recovery through magnetic separation was an efficient process. Previous studies also note that, while anatase nanoparticles can be reused in consecutive tests, the recovery of such particles is difficult, and the authors compared their separation with that of TiO_2 nanotubes, finding that the nanotubes could be much more easily recovered.[49,50] The inclusion of a magnetic core into the design of the particles presented in this work allows for the benefits of anatase nanoparticles to be retained while implementing a simple and efficient means of separation. Additionally, Yu and Xu[50] published results showing their nanorods to be separable within 1 h of gravimetric settling while magnetic separation presented in this work show magnetic particles to be separable in under a minute without the need for any filtration equipment. Furthermore, after the photocatalytic trials, aqueous solution containing the particles was transferred to a vial and placed next to a magnet. Complete separation of the particles from solution was achieved within 1 min of placing the vial adjacent to the magnet as seen in the inset of Figure 6, demonstrating that the magnetic response of the particles does not change with use.

4. CONCLUSIONS

Herein, an efficient hydrothermal treatment process was used to create hollow rattle-type particles, providing a simple method of attaining hollow structures which previously required more complicated synthesis routes. These rattle-type structures present a particle morphology superior to nonhollow spheres in terms of surface area and crystallinity while requiring only one additional step of processing. The use of hydrothermal dissolution of silica to selectively etch the silica spacer is a safe and efficient method of producing hollow, rattle-type particles of these materials and enables a quick, inexpensive, and simple alternative to the use of chemical etchants or organic templates. In addition to simplifying the synthesis, this hydrothermal treatment method introduces crystallinity to the TiO_2 outer layer, thereby simultaneously removing the spacer template while crystallizing the TiO_2. It is anticipated that, due to their good photocatalytic activity, simple and inexpensive synthesis methods, fast separation, and consistent recyclability, these particles will be highly applicable in large-scale future advanced water treatment.

■ ASSOCIATED CONTENT

Supporting Information

TEM images displaying the sampling areas for EDX characterization. This material is available free of charge via the Internet at http://pubs.acs.org.

■ AUTHOR INFORMATION

Corresponding Author

*Address: Department of Chemical Engineering, 200 University Ave. W, Waterloo, ON, N2L3G1, Canada. Tel: (519) 888-4567 ext. 38605. Fax: (519) 888-4347. E-mail: frank.gu@uwaterloo.ca.

Notes

The authors declare no competing financial interest.

■ ACKNOWLEDGMENTS

We would like to thank the Canadian Centre for Electron Microscopy (CCEM) for their assistance in SEM imaging, HRTEM/EDX characterization, and HRTEM/SAED characterization.

■ REFERENCES

(1) Chen, X.; Mao, S. *Chem. Rev.* **2007**, *107*, 2891−2959.
(2) Fujishima, A.; Zhang, X.; Tryk, D. *Surf. Sci. Rep.* **2008**, *63*, 515−582.
(3) Hoffmann, M.; Martin, S.; Choi, W.; Bahnemann, D. *Chem. Rev.* **1995**, *95*, 69−96.
(4) Bolong, N.; Ismail, A.; Salim, M.; Matsuura, T. *Desalination* **2009**, *239*, 229−246.
(5) Fent, K.; Weston, A.; Caminada, D. *Aquat. Toxicol.* **2006**, *76*, 122−159.
(6) Shannon, M.; Bohn, P.; Elimelech, M.; Georgiadis, J.; Marinas, B.; Mayes, A. *Nature* **2008**, *452*, 301−310.
(7) Mills, A.; Davies, R. H.; Worsley, D. *Chem. Soc. Rev.* **1993**, *22*, 417−425.
(8) Pozzo, R. L.; Baltanas, M. A.; Cassano, A. E. *Catal. Today* **1997**, *39*, 219−231.
(9) Chong, M. N.; Jin, B.; Chow, C. W. K.; Saint, C. *Water Res.* **2010**, *44*, 2997−3027.
(10) Zainal, Z.; Hui, L. K.; Hussein, M. Z.; Taufiq-Yap, Y. H.; Abdullah, A. H.; Ramli, I. *J. Hazard. Mater.* **2005**, *125*, 113−120.
(11) Byrne, J. A.; Eggins, B. R.; Brown, N. M. D.; McKinney, B.; Rouse, M. *Appl. Catal., B: Environ.* **1998**, *17*, 25−36.
(12) Fabiyi, M. .; Skelton, R. . *J. Photochem. Photobiol., A: Chem.* **2000**, *132*, 121−128.
(13) Han, H.; Bai, R. *Ind. Eng. Chem. Res.* **2009**, *48*, 2891−2898.
(14) Watson, S.; Scott, J.; Beydoun, D.; Amal, R. *J. Nanopart. Res.* **2005**, *7*, 691−705.
(15) Polshettiwar, V.; Luque, R.; Fihri, A.; Zhu, H.; Bouhrara, M.; Bassett, J.-M. *Chem. Rev.* **2011**, *111*, 3036−3075.
(16) Liu, Y.; Yu, L.; Hu, Y.; Guo, C.; Zhang, F.; Lou, X. *Nanoscale* **2012**, *4*, 183−187.
(17) Liu, Y.; Zhou, L.; Hu, Y.; Guo, C.; Qian, H.; Zhang, F.; Lou, X. *J. Mater. Chem.* **2011**, *21*, 18359−18364.
(18) Kim, T. H.; Lee, K. H.; Kwon, Y. K. *J. Colloid Interface Sci.* **2006**, *304*, 370−377.
(19) Li, X.; Xiong, Y.; Li, Z.; Xie, Y. *Inorg. Chem.* **2006**, *45*, 3493−3495.
(20) Sun, C.; Liu, L.; Qi, L.; Li, H.; Zhang, H.; Li, C.; Gao, F.; Dong, L. *J. Colloid Interface Sci.* **2011**, *364*, 288−297.
(21) Zhang, Y.; Xu, S.; Luo, Y.; Pan, S.; Ding, H.; Li, G. *J. Mater. Chem.* **2011**, *21*, 3664−3671.
(22) Yin, Y.; Zhou, S.; Min, C.; Wu, L. *J. Colloid Interface Sci.* **2011**, *361*, 527−533.
(23) Subagio, D. P.; Srinivasan, M.; Lim, M.; Lim, T.-T. *Appl. Catal., B: Environ.* **2010**, *95*, 414−422.
(24) Lou, X. W.; David; Archer, L. A.; Yang, Z. *Adv. Mater.* **2008**, *20*, 3987−4019.
(25) Agrawal, M.; Gupta, S.; Pich, A.; Zafeiropoulos, N. E.; Rubio-Retama, J.; Jehnichen, D.; Stamm, M. *Langmuir* **2010**, *26*, 17649−17655.
(26) Chen, J. S.; Chen, C.; Liu, J.; Xu, R.; Qiao, S. Z.; Lou, X. W. *Chem. Commun.* **2011**, *47*, 2631−2633.
(27) Liu, H.; Jia, Z.; Ji, S.; Zheng, Y.; Li, M.; Yang, H. *Catal. Today* **2011**, *175*, 293−298.
(28) Deng, Y.; Wang, C.; Hu, J.; Yang, W.; Fu, S. *Colloids Surf., A: Physicochem. Eng. Aspects* **2005**, *262*, 87−93.
(29) Luo, B.; Song, X.-J.; Zhang, F.; Xia, A.; Yang, W.-L.; Hu, J.-H.; Wang, C.-C. *Langmuir* **2010**, *26*, 1674−1679.
(30) Cheng, W.; Tang, K.; Sheng, J. *Chem.—Eur. J.* **2010**, *16*, 3608−3612.
(31) Cheng, W.; Tang, K.; Qi, Y.; Sheng, J.; Liu, Z. *J. Mater. Chem.* **2010**, *20*, 1799−1805.

(32) Lee, J.; Othman, M.; Eom, Y.; Lee, T.; Kim, W.; Kim, J. *Microporous Mesoporous Mater.* **2008**, *116*, 561−568.
(33) Ye, M.; Zhang, Q.; Hu, Y.; Ge, J.; Lu, Z.; He, L.; Chen, Z.; Yin, Y. *Chem.—Eur. J.* **2010**, *16*, 6243−6250.
(34) Kim, D.; Kwak, S. *Appl. Catal., A* **2007**, *323*, 110−118.
(35) Qi, G.; Liu, Y.; Jiao, W.; Zhang, L. *Micro Nano Lett.* **2010**, *5*, 278−281.
(36) Yavuz, C.; Mayo, J.; Yu, W.; Prakash, A.; Falkner, J.; Yean, S.; Cong, L.; Shipley, H.; Kan, A.; Tomson, M.; Natelson, D.; Colvin, V. *Science* **2006**, *314*, 964−967.
(37) Yu, Q.; Wang, P.; Hu, S.; Hui, J.; Zhuang, J.; Wang, X. *Langmuir* **2011**, *27*, 7185−7191.
(38) Alexander, G. B.; Heston, W. M.; Iler, R. K. *J. Phys. Chem.* **1954**, *58*, 453−455.
(39) Fu, X.; Clark, L. A.; Yang, Q.; Anderson, M. A. *Environ. Sci. Technol.* **1996**, *30*, 647−653.
(40) Jin, Y.; Li, A.; Hazelton, S. G.; Liang, S.; John, C. L.; Selid, P. D.; Pierce, D. T.; Zhao, J. X. *Coord. Chem. Rev.* **2009**, *253*, 2998−3014.
(41) Kim, S. K.; Chang, H.; Cho, K.; Kil, D. S.; Cho, S. W.; Jang, H. D.; Choi, J.-W.; Choi, J. *Mater. Lett.* **2011**, *65*, 3330−3332.
(42) Reyes-Coronado, D.; Rodriguez-Gattorno, G.; Espinosa-Pesqueira, M.; Cab, C.; De Coss, R.; Oskam, G. *Nanotechnology* **2008**, *19*, 145605.
(43) Yanagisawa, K.; Yamamoto, Y.; Feng, Q.; Yamasaki, N. *J. Mater. Res.* **1998**, *13*, 825−829.
(44) Li, S.; Shen, Q.; Zong, J.; Yang, H. *J. Alloys Compd.* **2010**, *508*, 99−105.
(45) Yu, J.; Wang, G.; Cheng, B.; Zhou, M. *Appl. Catal., B: Environ.* **2007**, *69*, 171−180.
(46) Beydoun, D.; Amal, R.; Low, G.; McEvoy, S. *J. Phys. Chem. B* **2000**, *104* (18), 4387−4396.
(47) Leshuk, T.; Linley, S.; Baxter, G.; Gu, F. *ACS Appl. Mater. Interfaces* **2012**, *4* (11), 6062−6070.
(48) Wu, W.; Xiao, X.; Zhang, S.; Ren, F.; Jiang, C. *Nanoscale Res. Lett.* **2011**, *6*, 533.
(49) Costa, L. L.; Prado, A. G. S. *J. Photochem. Photobiol., A: Chem.* **2009**, *201*, 45−49.
(50) Yu, Y.; Xu, D. *Appl. Catal., B: Environ.* **2007**, *73*, 166−171.